

Effects of Flow Variations on the Galvanic Corrosion of the Copper/AISI 304 Stainless Steel Pair in Lithium Bromide Using a Zero-Resistance Ammeter

M.T. Montañés, R. Sánchez-Tovar, J. García-Antón, V. Pérez-Herranz*

Ingeniería Electroquímica y Corrosión (IEC). Departamento de Ingeniería Química y Nuclear.
Universitat Politècnica de València, 46022, Valencia. Spain

*E-mail: jgarciaa@iqn.upv.es

Received: 20 October 2011 / *Accepted:* 2 December 2011 / *Published:* 1 January 2012

The effects of flow variations on the galvanic corrosion of the copper/AISI 304 stainless steel pair in a concentrated lithium bromide solution were investigated in a hydraulic circuit applying different flow steps and using a zero-resistance ammeter (ZRA). The flow steps consist in applying a flow rate for sixty minutes after leaving the system under stagnant conditions for another sixty minutes; this procedure is repeated during eight hours. The magnitude of the steps is different depending on the flow regime studied, ranging from a Reynolds number of 633 to 5066. Results show that, when a flow step is applied, the galvanic current density increases and the galvanic potential shifts towards more negative values. However, with time, this increase in the galvanic current density is lower, reaching its lowest value in the last hour of the experiment at a Reynolds number of 5066. Thus, although the corrosion rate increases as Reynolds number increases, the protective corrosion products are generated earlier on the copper surface.

Keywords: copper, stainless steel, lithium bromide, zero-resistance ammeter, hydrodynamic corrosion.

1. INTRODUCTION

The use of a zero-resistance ammeter (ZRA) allows registering the naturally occurring fluctuations in the potential and current of corroding electrodes that take place during a corrosion process [1]. Nowadays, this technique is gaining importance because it can be used without disturbing the system under investigation and in continuous-time [2]. Moreover, as it is a non-destructive technique, the results obtained are close to reality. However, there are only few works that have studied corrosion processes under flowing conditions by means of a ZRA [3-6]. Fluid flow can enhance corrosion problems [7-9] and this fact can have special importance in the regular stops of the

industries, due to maintenance and mechanical failure, where fluid flow can vary significantly. Galvanic corrosion studies that took into consideration flow variations using a ZRA are scarce [10-14]. Additionally, these studies made use of rotating electrodes in order to simulate a hydrodynamic regime, but these electrodes do not effectively simulate what really occurs in the industrial environment of interest. For this reason, in a previous work [15], a hydraulic circuit was used to investigate the galvanic corrosion of the copper/AISI 304 stainless steel pair in a concentrated lithium bromide solution under flowing conditions by means of a ZRA.

Lithium Bromide (LiBr) is one of the most commonly employed absorbents in absorption systems [16, 17], because of its good properties [18, 19]. Absorption machines are an alternative refrigeration technology to compression systems due to the fact that compression technology uses refrigerants that belong to the chlorofluorocarbon (CFC) group and, according to Montreal Protocol (1987), they are prohibited [20]. Furthermore, their substitutes, i.e. hydrochlorofluorocarbons, are submitted to severe regulations (Kyoto Protocol, 1997), since they are responsible for the ozone layer depletion and the climate change [21]. However, bromides are very aggressive ions that can cause serious corrosion problems on metallic components in absorption machines [22-24]. Copper and stainless steels are the most commonly used materials in absorption systems [25] because highly alloyed steels, which are supposed to cause less corrosion problems, are very expensive and usually have heat transfer problems. Copper is widely used in heat exchanger piping due to its high thermal conductivity and its good corrosion resistance [26-30], and stainless steels (i.e. AISI 304 stainless steel) are widely used in the structural elements of absorption refrigeration systems [31] because they present better corrosion resistance due to the chromium oxide film that protects the alloy [32, 33]. Therefore, copper provides AISI 304 stainless steel cathodic protection by acting as sacrificial anode; that is, copper is subjected to corrosion by the galvanic anodic dissolution effect [34].

The purpose of the present work was to investigate the effects of flow variations on the galvanic current density and galvanic potential of the copper/AISI 304 stainless steel pair in an 850 g/L LiBr solution applying different flow steps and using a zero-resistance ammeter (ZRA) in a hydraulic circuit. The flow steps consist in applying a flow rate for sixty minutes after leaving the system under stagnant conditions for another sixty minutes; this procedure is repeated for eight hours, simulating the possible stops of absorption machines, due to maintenance and mechanical failure, and subsequent starts. The magnitude of the steps is different depending on the flow regime studied, ranging from a Reynolds number of 633 to 5066.

2. EXPERIMENTAL PROCEDURE

2.1. Materials and solution

The galvanic pair used in this work consisted of copper and AISI 304 stainless steel. Copper composition was 99.9 wt. % and AISI 304 stainless steel composition is shown in Table 1. The copper and AISI 304 stainless steel rings were used in their as-received conditions [35]. They were only degreased with ethanol and air-dried prior to exposure. Both metal ring dimensions were identical to

avoid the effect of the cathode/anode area ratio in the galvanic study.

Table 1. Composition (wt.%) of AISI 304 stainless steel used in this work according to the inspection certificate supplied by the manufacturer.

C	Cr	Ni	Mn	Si	S	P	Fe
0.040	18.080	8.030	1.210	0.300	0.001	0.027	Bal.

The test solution was prepared by dissolving reagent grade LiBr (98 wt. %) in distilled water. Its concentration was 850 g/L, like the commercial solutions commonly used in absorption machines. Nitrogen was bubbled into the solution during 60 minutes in order to simulate oxygen-absence conditions in these machines, according to ASTM G5 [36]. Moreover, nitrogen was also bubbled when the solution was inside the hydrodynamic circuit during 20 minutes. Then, the hydrodynamic circuit was tight sealed to keep these conditions. The tests were performed at 25° C.

2.2. Hydrodynamic conditions

A hydraulic circuit was designed to carry out the experiments and it was described elsewhere [15]. It consisted of a centrifugal pump, a flow-meter, a glass device for the reference electrode, a glass device for a thermometer to control the temperature, a glass device for the gas output, a glass device to introduce the solution into the flow circuit, a glass device to bubble an inert gas, a thermostat to regulate the solution temperature and a valve to drain the system. Silicone flexible tubes were used to assemble the different elements. The test section was composed of two rings 20 mm in length and 14 mm in inner diameter, made of AISI 304 stainless steel (located at the flow inlet) and copper, respectively. Both rings were insulated by a Teflon intermediate assembly piece, which was 14 mm in inner diameter too. Fully developed flow was assured using a 90-cm-long Teflon rigid tube of the same inner diameter as the test rings upstream of the test section and a 20-cm-long Teflon rigid tube downstream of the test section.

In order to evaluate the effects of flow variations (i.e. possible stops of the machines, due to maintenance and mechanical failure, and subsequent starts), different flow steps were applied. The flow steps consist in applying a constant flow rate for sixty minutes after leaving the system under stagnant conditions for another sixty minutes; this procedure was repeated for eight hours. The magnitude of the steps was different depending on the flow regime studied, ranging from a Reynolds number of 633 to 5066. Furthermore, in order to evaluate the combined influence of time and flow, different magnitudes of flow steps were applied every hour during 10 hours. In this last case, Reynolds number ranged from 0 to 5066. The Reynolds number (Re) is a dimensionless group defined by the following equation:

$$\text{Re} = \frac{v \cdot d \cdot \rho}{\mu} \quad (1)$$

where v is the characteristic fluid velocity, d is the characteristic length of the system (the diameter of a pipe in the case of pipe flow), ρ is the fluid density and μ is the fluid viscosity. The LiBr solution density and viscosity were calculated according to the Patterson and Perez-Blanco numerical fits [37]; the obtained values were 1.59 g/cm^3 and 4.64 cP , respectively.

2.3. ZRA measurements

Galvanic current density and galvanic potential of the copper/AISI 304 stainless steel pair were measured every 0.5 s during 8 h using a zero-resistance ammeter (ZRA). Both copper and AISI 304 stainless steel rings were connected to a Solartron 1285 potentiostat, which was used as a ZRA and was provided with the Corrware software. The reference electrode was a silver/silver chloride (Ag/AgCl), 3 M potassium chloride (KCl) electrode.

According to the electrical measurements carried out, the current sign was positive when electrons flowed from the copper ring to the potentiostat; thus, copper was corroding. However, current values were negative when electrons flowed in the opposite direction, that is, AISI 304 stainless steel was corroding. In all cases, the tests were repeated at least three times in order to verify reproducibility. After each experiment, the test section was disassembled and the rings were washed with distilled water, rinsed with ethanol and air-dried. Then, they were cut in order to observe their internal surface.

3. RESULTS AND DISCUSSION

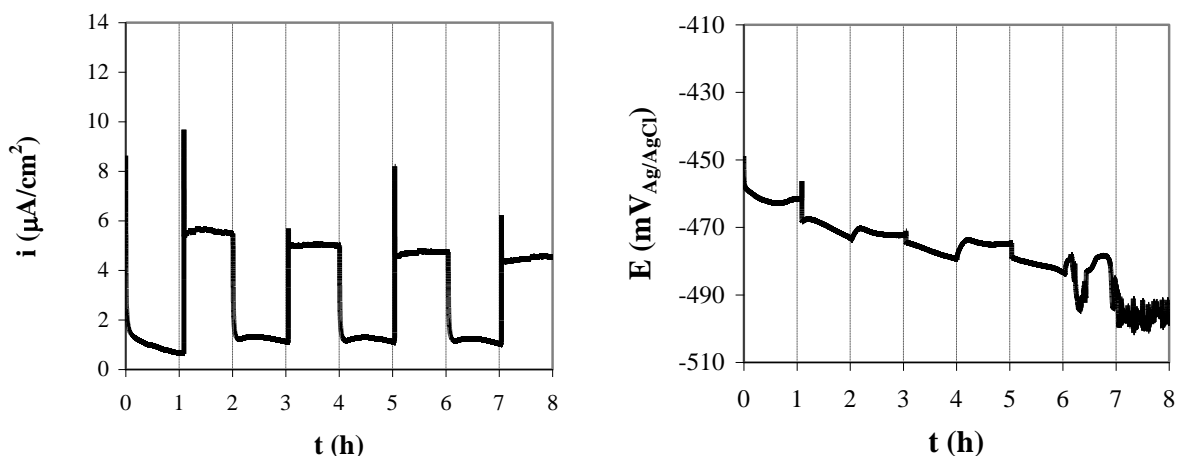
3.1. Analysis of the galvanic current density and galvanic potential profiles

Figure 1 shows the galvanic current density and galvanic potential profiles of the copper/AISI 304 stainless steel pair at the different studied flow steps. The positive current density values registered mean that copper is the anodic member of the pair for the three flow steps applied; so, copper corrodes in all cases while AISI 304 stainless steel remains protected.

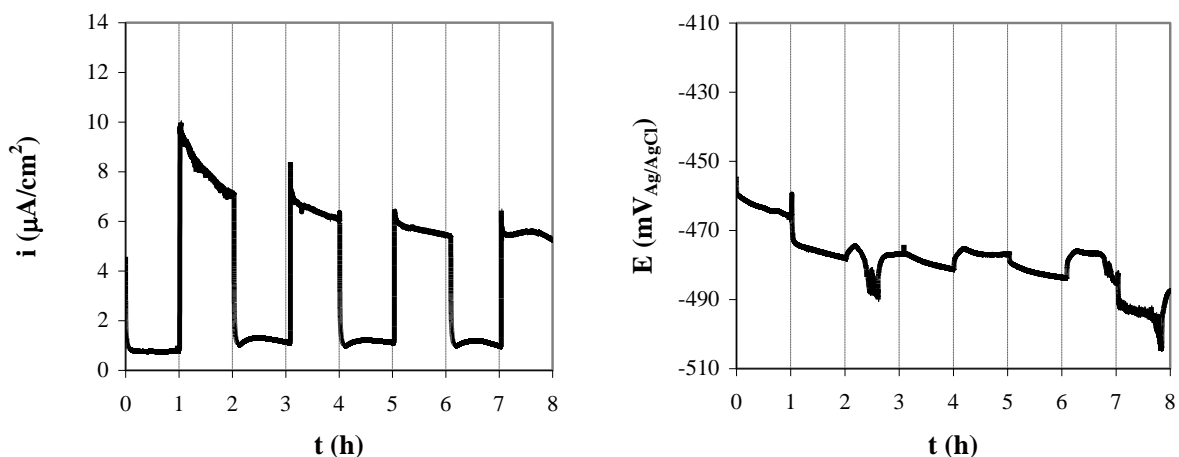
3.1.1. Galvanic current density profiles

The galvanic current densities show a general tendency to drastically increase when a flow step is applied. During the sixty minutes in which the flow step is applied at the highest studied Reynolds numbers (from Re 0 to Re 3166 and to Re 5066 in Figures 1b and 1c), the galvanic current density decreases with time. In the experience carried out at a flow step from Re 0 to Re 633, the galvanic current density values remain nearly constant after the application of a flow step. When a flow step is applied again, the galvanic current density initial value is practically equal to the last value registered at the previous flow step; that is, there is a complete recovery, except in the experience carried out at a flow step from Re 0 to Re 633 (Figure 1a), where the galvanic current density initial value is lower than the last value registered at the previous flow step.

(a) Flow step from Re = 0 to Re = 633



(b) Flow step from Re = 0 to Re = 3166



(c) Flow step from Re = 0 to Re = 5066

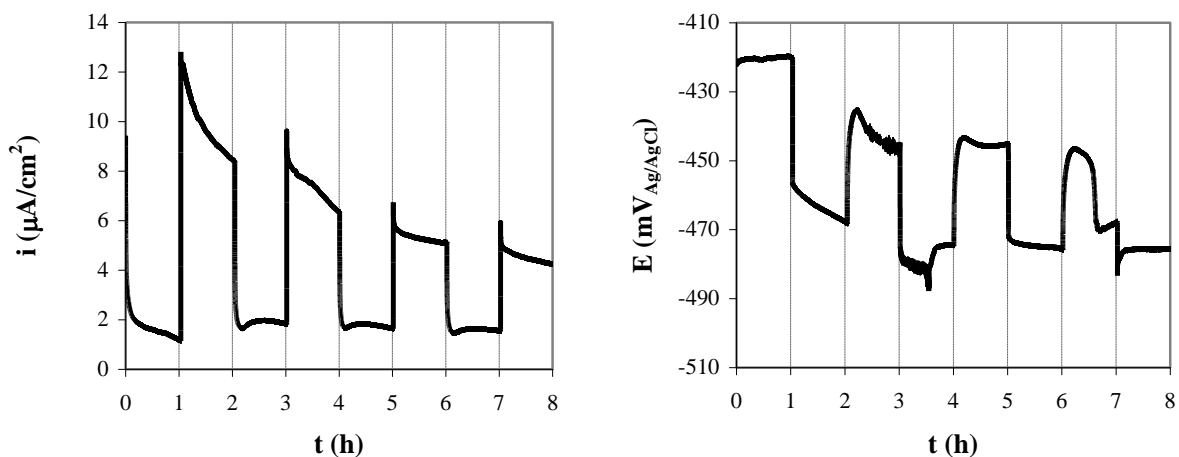


Figure 1. Galvanic current density and galvanic potential profiles of the copper/AISI 304 stainless steel pair at different flow steps during eight hours. (a) From Re = 0 to Re = 633. (b) From Re = 0 to Re = 3166. (c) From Re = 0 to Re = 5066.

In any case, the galvanic current density decreases with time. This decrease in galvanic current density can be attributed to metal passivation due to the formation of a protective film which grows with time [38]. On the other hand, when the pump is disconnected, a general tendency of the galvanic current density to sharply decrease can also be observed. Figure 1 also shows that during the sixty minutes in which the pump is disconnected, the galvanic current density initially increases with time due to inertia and then it decreases until it reaches the same initial value. Moreover, when the pump is disconnected again, the galvanic current density value is practically equal to the last value registered at the previous pump stop; that is, there is a complete recovery. However, there is an exception: the galvanic current density does not recover the last value registered during the first hour. Therefore, the first flow step alters the system.

3.1.2. Galvanic potential profiles

In relation to the galvanic potentials, their general tendency is to shift towards more negative values when a flow step is applied and to shift towards more positive values when the pump is disconnected. This behavior agrees with the registered galvanic current density values that are greater when a flow step is applied. Similarly to the galvanic current density profiles, the recovery of the galvanic potential values is practically complete, except for the last value registered during the first hour, showing that the first flow step alters the system.

3.2. Effect of Reynolds number on galvanic current density and galvanic potential

Although the general tendency of the galvanic current density and galvanic potential is similar when a flow step is applied, there are some differences depending on the magnitude of the applied step. In this way, in order to study the Reynolds number effect, Figure 2 shows the galvanic current density and the galvanic potential profiles of the copper/AISI 304 stainless steel pair at all flow steps applied.

3.2.1. Effect of Reynolds number on the galvanic current density

According to Figure 2a, when a flow step is applied, the effect of Reynolds number is to increase the galvanic current density value during the first hours of the test. Therefore, it can be said that during this period of time, the effect of galvanic coupling is greater at the highest Reynolds number. However, this behavior changes with time because when the third flow step is applied (sixth hour of the ZRA measurements), the galvanic current density is greater at a flow step from Re 0 to Re 3166 than those determined at a flow step from Re 0 to Re 5066. Moreover, when the fourth step is applied (last hour of the test) the galvanic current density is even lower at a flow step from Re 0 to Re 5066 than the register corresponding to a flow step from Re 0 to Re 633. This fact can be attributed to the quick and large formation of corrosion products that protect the copper ring at the highest flow.

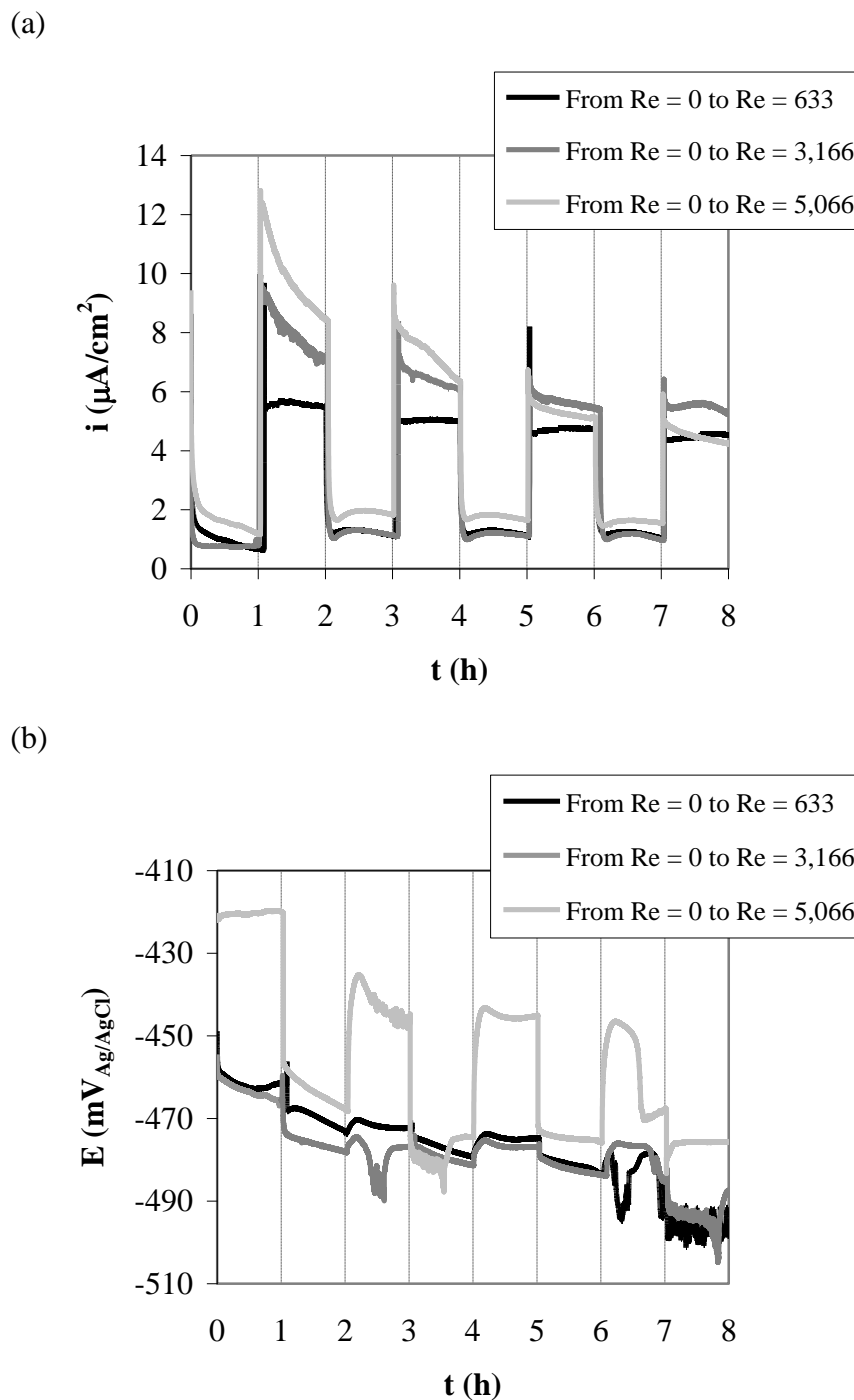


Figure 2. Effect of Reynolds number on galvanic current density (a) and galvanic potential (b) profiles of the copper/AISI 304 stainless steel pair applying different flow steps during eight hours.

Figure 2a also shows that when the pump is disconnected, the galvanic current density values are similar, regardless of the previous flow step applied. But, as it can be seen, there is an exception: when the previous flow step applied goes from Re 0 to Re 5066, the galvanic current density value is greater. This fact can be attributed to a greater inertia for the highest Reynolds number. However, with time, the difference decreases.

On the other hand, to study the effect of Reynolds number on the galvanic current density of the pair, a general dependence of the corrosion rate on fluid velocity could be established in terms of a potential relation between the corrosion rate and the Reynolds number [39-42]:

$$i = \text{constant} \cdot \text{Re}^a \tag{2}$$

The experimental exponent *a* in Equation 2 can be in the range from 1 to 3, depending upon the corrosion mechanism and flow regime. For simple mass transport to the inside wall of a tube, the value of exponent *a* is close to 1, while for erosion-corrosion in particle-containing liquids, the value is up to 3. For values between 1 and 3, there is a mixed control of mass transport and erosion-corrosion. For mixed control of a chemical step and mass transport, it varies between 0 and 1, depending on the mass transport [39, 41-44].

Mean galvanic current density values have been plotted according to Equation 2 in Figure 3 for the different hours at which a flow step was applied (second, fourth, sixth and eighth hours of the test).

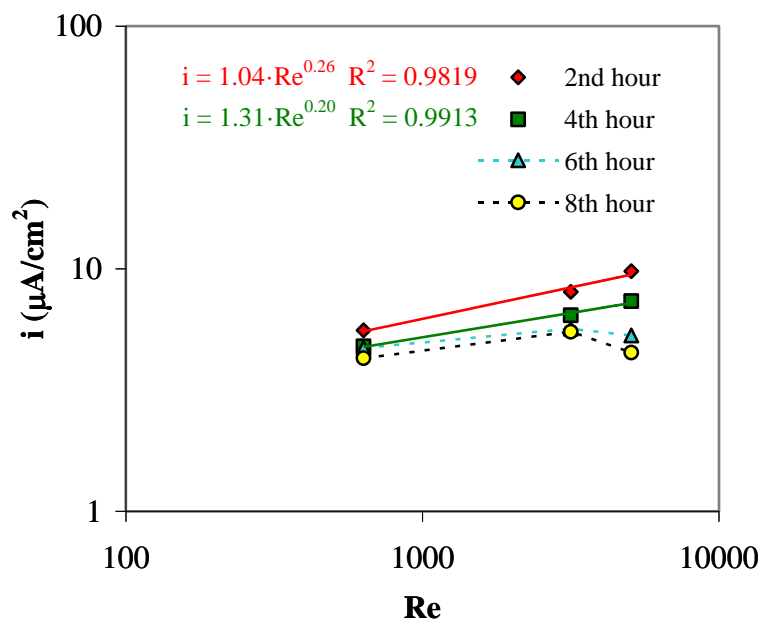


Figure 3. Variation of the mean galvanic current density of the copper/AISI 304 stainless steel pair with Reynolds number at the different hours when a flow step is applied.

Figure 3 shows that the least-square fitting of the experimental data was only possible for the second and fourth hours of the tests, since from this time the galvanic current densities obtained when a flow step is applied from Re 0 to Re 5066 is lower than that corresponding to the Re-0-to-Re-3166 step. Moreover, the experimental values of the galvanic current density for the second and fourth hours of the test fit Equation 2 well. The value of exponent *a* (0.26 and 0.20 for the second and fourth hours of the test, respectively) reveals that for the galvanic corrosion of the copper/AISI 304 stainless steel pair in LiBr there is a mixed control of a chemical step and mass transport with predominance of the former.

3.2.2. Effect of Reynolds number on the galvanic potential

Figure 2b shows the effect of the Reynolds number on the galvanic potential profiles. In this way, it can be observed in Figure 2b that when a flow step is applied or the pump is disconnected, differences between the reached galvanic potential values diminish with time. This fact agrees with the behavior observed for the galvanic current density.

Figure 2b also shows that when flow steps are applied from Re 0 to Re 5066, changes in the galvanic potential are much more accused, in relation to those corresponding to the other studied Reynolds numbers.

3.3. Materials examination

After each experiment, copper and AISI 304 stainless steel rings were cut in order to observe the corrosion process on their surface.

As it was previously pointed out, AISI 304 stainless steel remains protected from corrosion by copper that is why its inner surface, which was in contact with the LiBr solution, does not present corrosion damage in any case.

Figure 4 shows the images of the copper surface after the tests.

(a) From Re = 0 to Re = 633



(b) From Re = 0 to Re = 3166



(c) From Re = 0 to Re = 5066



Figure 4. Images of the copper surface after the tests: when a flow step is applied (a) from Re = 0 to Re = 633, (b) from Re = 0 to Re = 3166 and (c) from Re = 0 to Re = 5066.

Figure 4 reveals that copper undergoes uniform corrosion [45] and, in all the cases, the copper samples have lost their typical luster due to the corrosion process.

3.4. Combined influence of time and flow on the galvanic current density and galvanic potential

According to Figures 1 and 2, it seems that time has a great influence on the galvanic current density values. In order to corroborate this fact, an experiment consisting in applying different magnitude of flow steps every hour during 10 hours was carried out. The test started with the pump disconnected, and then a flow step from Re 0 to Re 633 was applied for the next hour. The flow was increased the same magnitude every hour during 9 hours. Therefore, the Reynolds number varies from 0 to 5066 in this experiment. During the last hour of the test, the pump was disconnected in order to study the recovery of the galvanic current density and galvanic potential. Figure 5 shows the galvanic current density and galvanic potential profiles obtained during the ten hours of the experiment. As in the other experiments carried out in this paper, the positive current density values registered mean that copper is the anodic member of the pair at all flow steps applied; therefore, AISI 304 stainless steel remains protected.

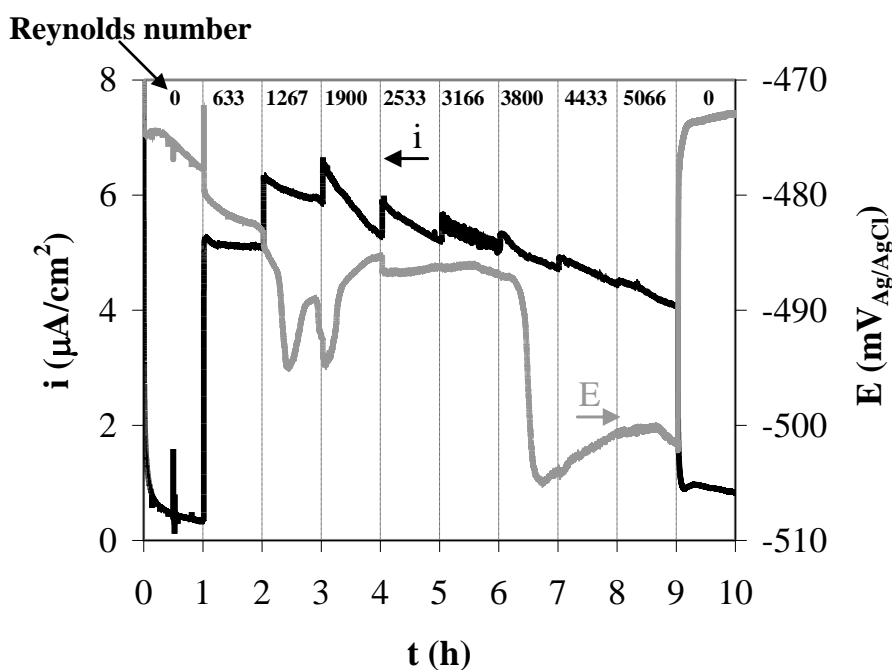


Figure 5. Combined influence of time and flow on galvanic current density and galvanic potential profiles of the copper/AISI 304 stainless steel pair applying different flow steps during ten hours.

It can be observed that the general tendency of the galvanic current density is to increase when a flow step is applied; that is, the corrosion rate increases with fluid flow [9]. However, with time, the increase in galvanic current density is lower than that registered in the previous hour. After the initial increase produced by the flow step, the galvanic current density diminishes during the rest of the hour. Figure 5 shows that the greater increase in the galvanic current density occurs during the second hour (when the first flow step is applied) and from the sixth to the ninth hour of the experiment, the galvanic current density hardly experiences any increase when a flow step is applied. This fact means that from

the sixth hour, the influence of time on the galvanic current density is greater than the influence of the fluid flow. Mansfeld [12-14] observed a similar behavior for aluminum coupled to copper in substitute ocean water: the galvanic current density increased with Reynolds number, but from a given Re the galvanic current density decreased due to the formation of corrosion products. Therefore, the results observed for copper coupled to AISI 304 stainless steel can be attributed to metal passivation due to the formation of a protective film which grows with time. Finally, when the pump is disconnected, the galvanic current density drastically decreases, but the value registered is greater than the last value obtained during the first hour; that is, the system recovery is not complete. However, the galvanic current density slightly diminishes with time trying to reach the initial value of the first hour of the test.

Figure 5 also shows that the general tendency of the galvanic potential is to shift towards more negative values when a flow step is applied. This fact agrees with the general tendency of the galvanic current density. At the end of the test, when the pump is disconnected, the galvanic potential sharply shifts towards more positive values that are similar to the values registered during the first hour; therefore, it can be said that the recovery of the galvanic potential is almost complete.

4. CONCLUSIONS

In this paper the effects of flow variations on galvanic current density and galvanic potential of the copper/AISI 304 stainless steel pair in a heavy LiBr brine have been studied by means of a zero-resistance ammeter (ZRA). The magnitude of the steps is different depending on the flow regime studied, ranging from a Reynolds number of 633 to 5066. A hydraulic circuit was used to study hydrodynamic corrosion *in situ* without breaking pipe continuity. The main findings of the work are presented below.

1. The results obtained from the open circuit measurements show that copper is the anodic member of the pair at all flow steps applied and it undergoes uniform corrosion losing its characteristic luster.
2. When a flow step is applied, galvanic current density tends to sharply increase. During the sixty minutes during which a flow step is applied, the galvanic current density decreases with time. This decrease can be attributed to metal passivation due to the formation of a protective film which grows with time. When a flow step is applied again, there is a complete recovery of the galvanic current density value for the higher Reynolds numbers.
3. When the pump is disconnected, the galvanic current density tends to sharply decrease. When the pump is disconnected again, there is a complete recovery of the galvanic current density value, excepting the recovery of the last value registered during the first hour.
4. Exponent n applied to the Reynolds number could only be calculated for the second and fourth hours of the tests showing a mixed control of a chemical step and mass transport for the galvanic corrosion of the copper/AISI 304 stainless steel pair, with predominance of the former.
5. The galvanic potential tends to shift towards more negative values when a flow step is applied and to shift towards more positive ones when the pump is disconnected. This behavior agrees

with the registered values of the galvanic current density. Furthermore, the recovery of the galvanic potential values is almost complete.

6. The galvanic current density is greater when the Reynolds number increases. However, this behavior changes with time. This fact can be attributed to the quick and large formation of corrosion products that protect the copper ring at the highest flow rates.
7. From a given hour, the influence of time on the galvanic current density is greater than the effect of fluid flow.

ACKNOWLEDGMENTS

The authors would like to express their gratitude to the MICINN for the financial support (project CTQ2009-07518), to the FPU grant given to Rita Sánchez Tovar, to FEDER (Fondo Europeo de Desarrollo Regional) and to Dr. Asunción Jaime for her translation assistance.

References

1. J.R. Kearns, J.R. Scully, P.R. Roberge, D.L. Reichert, J.L. Dawson, *Electrochemical Noise Measurement for Corrosion Applications*, ASTM, STP 1227, Philadelphia (1996).
2. M.G. Pujar, N. Parvathavarthini, R.K. Dayal and H.S. Khatak, *Int. J. Electrochem. Sci.*, 3 (2008) 44.
3. J.A. Wharton, R.J.K. Wood, *Corrosion*, 61 (2005) 792.
4. J.A. Wharton, R.J.K. Wood, *Wear*, 256 (2004) 525.
5. X.Y. Zhou, S.N. Lvov, X.J. Wei, L.G. Benning, D.D. Macdonald, *Corros. Sci.*, 44 (2002) 841.
6. R.J.K. Wood, J.A. Wharton, A.J. Speyer and K.S. Tan, *Tribol. Int.*, 35 (2002) 631.
7. A.Y. Musa, A.A.H. Kadhum, A. Bakar-Mohamad, A. Razak-Daud, M. Sobri-Takriff, S. Kartom-Kamarudin and N. Muhamad, *Int. J. Electrochem. Sci.*, 4 (2009) 707.
8. J. Mendoza-Canales and J. Marín-Cruz, *Int. J. Electrochem. Sci.*, 3 (2008) 346.
9. T.Y. Chen, A.A. Moccari, D.D. Macdonald, *Corrosion*, 48 (1992) 239.
10. G. Kear, B.D. Barker, K.R. Stokes and F.C. Walsh, *Corros. Sci.*, 47 (2005) 1694.
11. J.A. Wharton, R.C. Barik, G. Kear, R.J.K. Wood, K.R. Stokes and F.C. Walsh, *Corros. Sci.*, 47 (2005) 3336.
12. F. Mansfeld, J. V. Kenkel, *Corrosion*, 33 (1977) 236.
13. F. Mansfeld, J. V. Kenkel, *Corrosion*, 33 (1977) 376.
14. F. Mansfeld, *Corrosion*, 32 (1976) 380.
15. M.T. Montañés, R. Sánchez-Tovar, J. García-Antón, V. Pérez-Herranz, *Int. J. Electrochem. Sci.*, 5 (2010) 1934.
16. R.J. Romero, P.M.A. Basurto, H.A.H. Jiménez, M.J.J. Sánchez, *Sol. Energy*, 80 (2006) 177.
17. W. Riviera, R.J. Romero, M.J. Cardoso, J. Aguillón, R. Best, *Int. J. Energ. Res.*, 26 (2002) 747.
18. J.W. Furlong, *The Air Pollution Consultant*, 11/12 (1994) 1.12.
19. K. Tanno, M. Itoh, T. Takahashi, H. Yashiro and N. Kumagai, *Corros. Sci.*, 34 (1993) 1441.
20. *Official J.*, L 297 (1988) 8.
21. *Official J.*, L 130 (2002) 1.
22. E. Sarmiento, J.G. González-Rodríguez, J. Uruchurtu, O. Sarmiento and M. Menchaca, *Int. J. Electrochem. Sci.*, 4 (2009) 144.
23. X. Hu, C. Liang, *Mater. Chem. Phys.*, 110 (2008) 285.
24. V. Oleinik, I.K. Yu, A.R. Vartapetyan, *Prot. Met.*, 39 (2003) 12.
25. G.A. Florides, S.A. Kalogirou, S.A. Tassou, L.C. Wrobel, *Energy Conv. Manag.*, 44 (2003) 2483.
26. L. Nuñez, E. Reguera, F. Corvo, E. Gonzalez, C. Vazquez, *Corros. Sci.*, 47 (2005) 461.

27. E.S.M. Sherif, R.M. Erasmus, J.D. Comins, *J. Colloid Interf. Sci.*, 309 (2007) 470.
28. A. Valero-Gomez, A. Igual-Munoz, J. Garcia-Anton, *Corrosion*, 62 (2006) 1117.
29. M.M. Antonijevic, G.D. Bogdanovic, M.B. Radovanovic, M.B. Petrovic and A.T. Stamenkovic, *Int. J. Electrochem. Sci.*, 4 (2009) 654.
30. M.M. Antonijevic, S.C. Alagic, M.B. Petrovic, M.B. Radovanovic and A.T. Stamenkovic, *Int. J. Electrochem. Sci.*, 4 (2009) 516.
31. D. Itzhak, O. Elias, *Corrosion*, 50 (1994) 131.
32. T. Bellezze, G. Roventi, R. Fratesi, *Electrochim. Acta*, 49 (2004) 3005.
33. M.J. Carmezim, A.M. Simoes, M.F. Montemor, M.D. Belo, *Corros. Sci.*, 47 (2005) 581.
34. O. Elias, G. Horovitz, Hyun M., D. Itzhak, *Proc. 7th Israeli Material Engineering Conf.* (Hifa, Israel (1994).
35. ASTM G-1, *Standard Practice for Preparing, Cleaning and Evaluating Corrosion Test Specimens*, ASM International, USA (1994).
36. ASTM G-5, *Test Method for Making Potentiostatic and Potentiodynamic Anodic Polarization measurements*, ASM International, USA (2004).
37. M. R. Patterson and H. Pérez-Blanco, *ASHRAE Trans.*, 94 (1988) 2059.
38. G.T. Burstein, C. Liu, R.M. Souto, *Biomaterials*, 26 (2005) 245.
39. E. Heitz, *Electrochim. Acta*, 41 (1996) 503.
40. E. Heitz, *Corrosion*, 47 (1991) 135.
41. M. M. Stack, F. H. Stott, G. C. Wood, *J. Phys. IV*, 3 (1993) 687.
42. J. R. Shadley, S. A. Shirazi, E. Dayalan, E. F. Rybicki, *Corrosion*, 54 (1998) 972.
43. M. M. Stack, J. G. ChaconNava, F. H. Stott, *Mater. Sci. Tech.*, 11 (1995) 1180.
44. J. R. Shadley, S. A. Shirazi, E. Dayalan, M. Ismail, E. F. Rybicki, *Corrosion*, 52 (1996) 714.
45. J. J. Shim, J. G. Kim, *Mater. Lett.*, 58 (2004) 2002.